

**Supplementary Information for “Non-Monotonic Evolution of  
Carrier Density and Mobility under Thermal Cycling Treatments in  
Dirac Semimetal Cd<sub>3</sub>As<sub>2</sub> Microbelts”**

Zheng Chen(陈正)<sup>1,2‡</sup>, Min Wu(武敏)<sup>1,2‡</sup>, Yequn Liu(刘叶群)<sup>3</sup>,  
Wenshuai Gao(高文帅)<sup>4</sup>, Yuyan Han(韩玉岩)<sup>1</sup>, Jianhui Zhou(周建辉)<sup>1,\*</sup>,  
Wei Ning(宁伟)<sup>1,\*</sup>, and Mingliang Tian(田明亮)<sup>1,4</sup>

<sup>1</sup> *Anhui Province Key Laboratory of Condensed Matter Physics at Extreme Conditions,  
High Magnetic Field Laboratory, Chinese Academy of Sciences, Hefei 230031,  
China.*

<sup>2</sup> *Department of physics, University of Science and Technology of China, Hefei  
230026, China.*

<sup>3</sup> *Analytical Instrumentation Center, State Key Laboratory of Coal Conversion,  
Institute of Coal Chemistry, Chinese Academy of Sciences, Taiyuan 030001, China.*

<sup>4</sup> *Department of Physics, School of Physics and Materials Science, Anhui University,  
Hefei 230601, China.*

<sup>‡</sup>Those authors contribute equally to this work.

<sup>\*</sup>To whom correspondence should be addressed. E-mail: jhzhou@hmfl.ac.cn;  
ningwei@hmfl.ac.cn (W.N.)

## 1. The carrier mobility and density

For a magnetic field perpendicular to the sample plane ( $\theta = 0^\circ$ ), the emergence of extra quantum oscillations in sample#1 at high fields without thermal cycling treatment (TCT), as shown in Fig. 2(a) of main text and Fig. S1(a), can be attributed to the surface Fermi-arcs participating in unusual Weyl magnetic orbits [1], and have been detailedly discussed in the main text. The Fermi-arc-mediated quantum oscillations are also observed in samples #2 and #3 with  $B > 6 T$  and  $B > 9 T$ , as plotted in Figs. S1(b) and S1(c), respectively.

Due to the suppression of backscattering by  $\pi$  Berry phase in topological semimetals with a  $k$ -linear dispersion, a high carrier mobility is expected. To obtain the mobility of  $\text{Cd}_3\text{As}_2$  microbelts, we have carried out the Hall resistivity measurements at  $T = 2 \text{ K}$  without TCT and the measured resistivity ( $\rho_{xx}$  and  $\rho_{xy}$ ), as plotted in Figs. S1(a)-S1(c), has been converted to the conductivity ( $\sigma_{xx}$  and  $\sigma_{xy}$ ), as depicted in Figs. S1(d)-S1(f). The carrier mobility can be estimated by standard Bloch-Boltzmann transport formula [2],  $\mu_1 = \mu_m \sqrt{\gamma}$ , where  $\mu_m = \sqrt{\mu_1 \mu_2} = \frac{1}{B_{max}}$  with  $B_{max}$  the field corresponding to the peak position of  $\sigma_{xy}(B)$  and  $\gamma = \rho_2 / \rho_1$  the resistivity anisotropy. The subscripts 1 and 2 refer to the current direction along the longitudinal and transverse directions, respectively. The resistivity anisotropy  $\gamma$  is about 25, as studied in our previous work [3]. The carrier mobility deduced from  $\mu_m$  is shown in Table 1 of main text, the obtained carrier mobility in our microbelts is comparable with previous studies of  $\text{Cd}_3\text{As}_2$  single crystals [2].

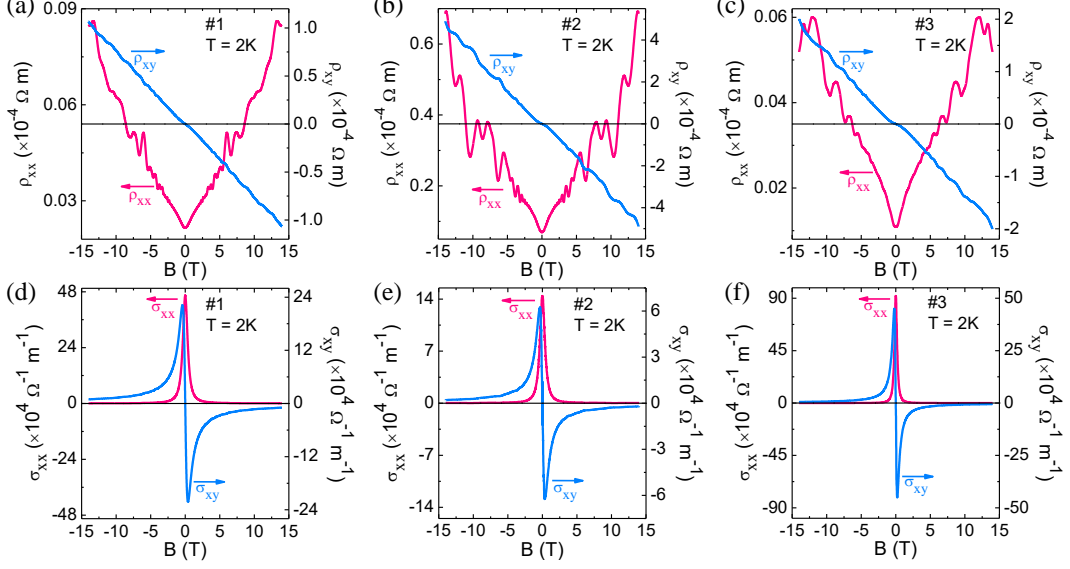


**Fig. S1.** (Color online) (a-c) The longitudinal magnetoresistivity and Hall resistivity for samples #1, #2 and #3 at  $T = 2$  K, respectively, without the TCT. (d-f) The corresponding longitudinal magnetoconductivity and Hall conductivity.

## 2. Negative longitudinal magnetoresistivity and Scattering time $\tau_c$

Another striking feature in Weyl/Dirac semimetals is the negative LMR, which is usually attributed to the chiral anomaly. While a temporarily upward-shifted Fermi level would suppress this negative LMR, due to the change of the band topology. We believe that after the fourth TCTs in sample #1, the Fermi energy is approaching the Lifshitz transition point where the single Fermi surface encloses two Dirac cones. This is well illustrated in our experiments, as we can see in Fig. S2(a), the negative LMR has been largely suppressed after four TCTs. In the picture of chiral anomaly, this can also be well identified via the intervalley scattering time  $\tau_c$  of chiral charges. According to the semi-classical transport theory [4], in weak field limit, the positive conductivity induced by chiral anomaly is proportional to  $B^2$ . Indeed, this quadratic field

dependence is consistent with our experimental observations in low magnetic fields, as shown in Fig. S2(b). Theoretically, the ratio between the chiral anomaly induced conductivity increment  $\delta\sigma_{xx}$  and zero field conductivity  $\sigma_0$  can be written as [4]:

$$\frac{\delta\sigma_{xx}}{\sigma_0} = \frac{3}{4} \frac{e^2 v_F^2}{E_F^2 k_F^2} B^2 \frac{\tau_c}{\tau_{tr}} \quad (1)$$

with  $\tau_{tr}$  the transport lifetime. Fitting the temperature-dependent oscillation amplitudes to the Lifshitz-Kosevich formula [5,6], we can get the effective mass which changes from  $0.039 m_e$  to  $0.043 m_e$  after the four TCTs. The transport lifetime can be deduced by the relationship  $\tau_{tr} = \mu \hbar k_F / e v_F$  with Fermi velocity  $v_F = \hbar k_F / m^*$ . Finally, we get the scattering time  $\tau_c$ , which decreases from  $4 \times 10^{-12} s$  to  $1.35 \times 10^{-12} s$  after four TCTs. The dramatic damping of the scattering time  $\tau_c$  gives another evidence that the upward shifting of the Fermi energy suppresses the chiral charge pumping in  $\text{Cd}_3\text{As}_2$  microbelts due to the change of the band topology.

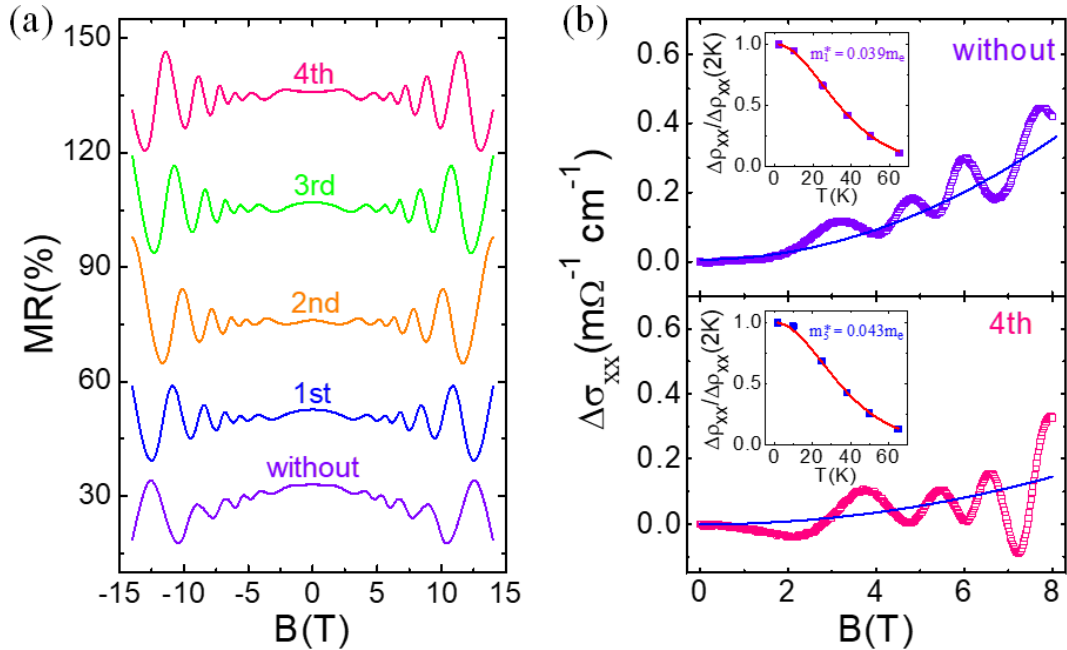


**Fig. S2.** (Color online) (a) The chiral anomaly induced negative LMR in parallel electromagnetic fields at  $T = 2$  K for each measurement with and without the TCTs

in sample #1. (b) The positive longitudinal magnetoconductivities before and after the TCTs at  $T = 2$  K. The blue curves are the fitting of the magnetoconductivity backgrounds to  $B^2$ -type function. Inset: The fittings of the temperature-dependent oscillation amplitudes to the Lifshitz-Kosevich formula generate the effective mass  $0.039 m_e$  and  $0.043 m_e$  before and after the TCTs, respectively.

## Reference

- [1] Potter AC, Kimchi I, Vishwanath A. Quantum oscillations from surface Fermi arcs in Weyl and Dirac semimetals. *Nat Commun* 2014;5:5161.
- [2] Liang T, Gibson Q, Ali MN, et al. Ultrahigh mobility and giant magnetoresistance in the Dirac semimetal  $\text{Cd}_3\text{As}_2$ . *Nat Mater* 2015;14:280-284.
- [3] Wu M, Zheng GL, Chu WW, et al. Probing the chiral anomaly by planar Hall effect in Dirac semimetal  $\text{Cd}_3\text{As}_2$  nanoplates. *Phys Rev B* 2018;98:161110(R).
- [4] Son DT, Spivak BZ. Chiral anomaly and classical negative magnetoresistance of Weyl metals. *Phys Rev B* 2013;88:104412.
- [5] Shoenberg D. *Magnetic Oscillations in Metals* (Cambridge University Press, Cambridge, England, 1984).
- [6] Murakawa H, Bahramy MS, Tokunaga M, et al. Detection of Berry's Phase in a Bulk Rashba Semiconductor. *Science* 2013;342:1490-1493.